J. Nanoanalysis., 9(4): 332-337, Autumn 2022

RESEARCH ARTICLE

Computational investigation of adsorption of Lewisite Warfare Agents on the $B_{12}N_{12}$ and $M^+@B_{12}N_{12}$ ($M^+ = Li^+, Na^+, K^+$) nanoclusters

Reza Ghiasi**, Rashin Emami, Maryam Vasfi Sofiyani

Department of Chemistry, East Tehran Branch, Islamic Azad University, Tehran, Iran

ARTICLE INFO

Article History:
Received 2022-04-10
Accepted 2022-07-24
Published 2022-12-22

Keywords:
B12N12 Cluster,
Lewisite,
Adsorption,
Molecular Orbital Analysis,
Population of Conduction Electrons,
Thermodynamics Parameters.

ABSTRACT

This research surveyed the adsorption of Lewisite warfare agent on the $B_{12}N_{12}$ and $M^+@B_{12}N_{12}$ ($M^+ = Li^+, Na^+, K^+$) nanoclusters with LC-wPBE/ 6-311+G(d,p) at the level of theory. Adsorption energy values of Lewisite on the nanoclusters were computed, and the impact of metal cation on the adsorption was uncovered. Thermodynamic parameters of these responses were computed. Molecular orbital analyses of the $B_{12}N_{12}$ … Lewisite and $M^+@B_{12}N_{12}$ …. Lewisite systems were explained.

How to cite this article
Ghiasi R., Emami R., Vasfi Sofiyani M., Computational investigation of adsorption of Lewisite Warfare Agents on the $B_{12}N_{12}$ and $M^+@B_{12}N_{12}$ ($M^+ = Li^+, Na^+, K^+$) nanoclusters. J. Nanoanalysis., 2022; 9(4): 332-337. DOI: 10.22034/jna.2022.1946948.1240

INTRODUCTION

Genuine health risks are made after the contamination of environment by chemical warfare agent (CWA). Among CWAs, trans-2-chlorovinyldichloroarsine, known as Lewisite (Lew-I), may be a capable rankling chemical warfare operator; the primary generation of this agent dates back to the conclusion of World War I and it caused serious chemical burns of the eyes, skin, and lungs [1]. For obtaining Lewisite, acetylene reacts with arsenic trichloride [2]. Trivalent arsenic is poisonous due to its reactivity with noteworthy organic sulfhydryls [3]. In World War II, British Anti-Lewisite, 2,3 dimerceptopropanol (H2DMPA, BAL), was connected as an antidote to the chemical weapon Lewisite, 2-chloroethenyldichloroarsine, the so-called "Dew of Death". Amazingly, the activity of this instrument at the molecular level and the coordination property of this conventional medicate towards various arsenicals are hazy. A few researches centered on the interaction of arsenous corrosive with the BAL demonstrated the structure and soundness of species made in a sudden complex system [4]. A research detailed computational examination of detoxification of Lewisite warfare operators by British anti-Lewisite [5]. Nano structures like fullerene empty nano-clusters of components other than carbon were favored due to their uncommon electronic and optical characteristics [6-9]. Group III-V nitrides are among the foremost profitable nano-clusters [10-14]. BN nanoclusters are the isostructural course of carbon bucky balls, arranged by chemical vapor testimony strategy [15]. These particles have been utilized for helpful purposes due to the biocompatibility [16].They are regarded to be challenge for carbon based fullerenes within the

---

* Corresponding Author Email: *rezaghiasi1353@yahoo.com*

following era gadgets. Arrangement of the $B_{12}N_{12}$ nanocluster was detailed by laser desorption time-of flight mass spectrometry [17, 18]. A few computational examinations were explained almost of intelligent between $B_{12}N_{12}$ cluster and different molecules [19-24].

This computational study regarded the interaction between $B_{12}N_{12}$ and $M^+@B_{12}N_{12}$ (M^+ = Li^+, Na^+, K^+) nanoclusters with Lewisite warfare agent at LC-wPBE/ 6-311+G(d,p) level of theory. The structural parameters, frontier orbital energies and thermodynamics parameters were computed. The impact of metal cation on the adsorption was outlined.

COMPUTATIONAL METHODS

Optimization and vibrational investigation were performed with Gaussian 09 software package [25]. The standard 6-311+G(d,p) basis set [26-28] were regarded. LC-wPBE functional (a long range-corrected adaptation of wPBE) [29] is the level of theory that most precisely explains the HOMO–LUMO gap. The identities of optimized structures as a vitality least were affirmed by vibrational analysis.

RESULTS AND DISCUSSION

Adsorption Energy Values

The most stable isomer of the adsorbed Lewisite on the $B_{12}N_{12}$ nano-cluster is displayed in Fig. 1. At that point, this isomer is doped with alkaline metal cations. Chosen metal cations are Li^+, Na^+, and K^+. Adsorption vitality values of the Lewisite particle on the $M^+@B_{12}N_{12}$ nano-clusters are recorded in Table 2. The adsorption energy value (ΔE_{ad}) is ordinarily computed as below:

$$\Delta E_{ad}=E(cluster...Lewisite)-E(cluster)-E(Lewisite)+E(BSSE)$$

Where, E (cluster) is the vitality of isolate cluster, E (Lewisite) is the energy of the separated Lewisite, and E (cluster…Lewisite) is the energy of Lewisite adsorbed on the cluster surface. E(BSSE) is the basis set superposition errors (BSSE), which was corrected for adsorption vitality [30, 31]. The large negative ΔE_{ads} shows the adsorption of Lewisite particle on the nano-clusters. It can be found that these adsorptions are vivaciously favorable. The adsorption energies showed that the doped nanoclusters have more propensities to adsorb Lewisite than $B_{12}N_{12}$ cluster. Adoption strength decreased with increasing of atomic number of metal cation.

Bond distances

B-C and N-C bond separations of Lewisite…$B_{12}N_{12}$ and Lewisite…$M^+@B_{12}N_{12}$ nano-clusters frameworks are recorded in Table 1. It can be found that B-C and N-C bonds within the Lewisite…$M^+@B_{12}N_{12}$ systems are longer than Lewisite…$B_{12}N_{12}$ system. B-C bond lengths decreased with increasing of atomic number of metals within the Lewisite…$M^+@B_{12}N_{12}$ systems. In contrast, N-C bond lengths increased with increasing of atomic number of metals within the Lewisite…$M^+@B_{12}N_{12}$ systems.

Molecular orbital analysis

The frontier orbitals energy values and the HOMO-LUMO gap values in $B_{12}N_{12}$ and $M^+@B_{12}N_{12}$ nano-clusters systems are recorded in Table 2. These values uncovered more stability of frontier orbital within the metal-doped clusters in comparison with exclusive cluster. On the other

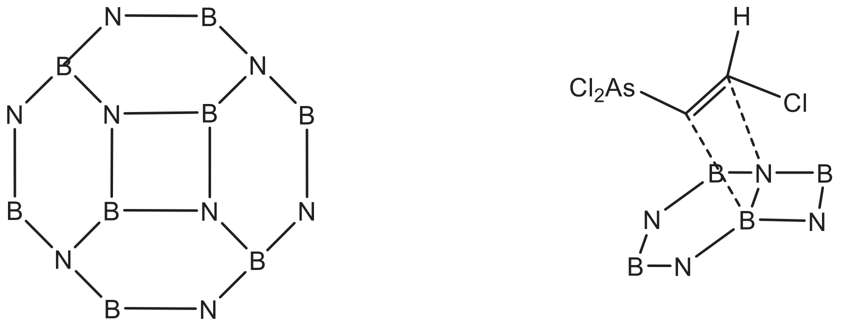

(a) (b)

Fig. 1. (a) Front view of the $B_{12}N_{12}$ nanocluster and (b) the most stable isomer of the adsorbed Lewisite on the $B_{12}N_{12}$ nanocluster.

Table 1. Adsorption energy (ΔE_{ads}, kcal/mol) values of Lewisite on the $B_{12}N_{12}$ and $M^+@B_{12}N_{12}$ (M^+=Li, Na, K) and B-C and N-C distances (Å) in the $M^+@B_{12}N_{12}$… Lewisite and $M^+@B_{12}N_{12}$… Lewisite systems at the LC-wPBE/ 6-311+G(d,p) level of theory.

Molecule	ΔE_{ads}	B-C	N-C
$B_{12}N_{12}$… Lewisite	-197.12	1.56829	1.44580
$Li^+@B_{12}N_{12}$… Lewisite	-232.74	1.58886	1.44998
$Na^+@B_{12}N_{12}$… Lewisite	-225.56	1.58693	1.45200
K^+ @$B_{12}N_{12}$… Lewisite	-225.20	1.58773	1.45382

Table 2. Frontier orbital energy and HOMO-LUMO gap values (eV) for $B_{12}N_{12}$, Lewisite, $M^+@B_{12}N_{12}$… Lewisite and $M^+@B_{12}N_{12}$… Lewisite systems at the LC-wPBE/6-311+G(d,p) level of theory.

Molecule	E(HOMO)	E(LUMO)	Gap
$B_{12}N_{12}$	-10.99	0.81	11.79
Lewisite	-10.51	0.01	10.52
$B_{12}N_{12}$… Lewisite	-10.49	0.21	10.70
$Li^+@B_{12}N_{12}$… Lewisite	-13.96	-3.76	10.20
$Na^+@B_{12}N_{12}$… Lewisite	-13.90	-3.72	10.18
K^+ @$B_{12}N_{12}$… Lewisite	-13.87	-3.79	10.08

Table 3. Thermodynamic parameters (kcal/mol) of adsorption Lewisite on the $B_{12}N_{12}$ and $M^+@B_{12}N_{12}$ (M^+=Li, Na, K)

Molecule	ΔG	ΔH	ΔS	K
$B_{12}N_{12}$… Lewisite	-14.11	-28.54	-48.41	2.22×10^{10}
$Li^+@B_{12}N_{12}$… Lewisite	-21.16	-36.60	-51.79	3.30×10^{15}
$Na^+@B_{12}N_{12}$… Lewisite	-21.40	-36.78	-51.59	4.94×10^{15}
K^+ @$B_{12}N_{12}$… Lewisite	-29.27	-44.74	-51.87	2.93×10^{21}

hand, HOMO-LUMO gap values are decreased within the $M^+@B_{12}N_{12}$ systems compared to $B_{12}N_{12}$ cluster. Plots of frontier orbital in e Lewisite…$B_{12}N_{12}$ and Lewisite…$Li^+@B_{12}N_{12}$ nano-clusters systems are displayed in Fig. 2. The significant contribution of Lewisite fragment can be observed within the frontier orbitals of these systems. Comparative plots were seen within the Lewisite…$Na^+@B_{12}N_{12}$ and Lewisite…$K^+@B_{12}N_{12}$ systems.

Population of conduction electrons

The population of conduction electrons (N) can be calculated with following equation:

$$N = A.T^{\frac{3}{2}}.\exp\left(-\frac{\Delta E_{gap}}{2k_B.T}\right)$$

In this equation, k_B, ΔE_{gap}, T and A are Boltzmann constant, HOMO-LUMO gap energy, temperature and a constanat (in electrons/m^3 $K^{3/2}$). ΔE_{gap} values were regarded as a reasonable parameter for the adsorbent affectability to an adsorbate. If ΔE_{gap} values drop, an exponential increment will happen within the populace of conduction electrons. The electron populace will ordinarily be modified into an electric flag. The magnitude of this signal might be ascribed to the nearness of Lewisite molecule. Hence, $B_{12}N_{12}$ and $M^+@B_{12}N_{12}$ nanoclusters can recognize the nearness of Lewisite by making an electrical noise.

Thermodynamic parameters

Free energy enthalpy and entropy changes (ΔG, ΔH and ΔS, respectively) of $B_{12}N_{12}$…Lewisite and $M^+@B_{12}N_{12}$… Lewisite complexes formation are computed in the basis of following reactions:

$B_{12}N_{12}$ + Lewisite → $B_{12}N_{12}$… Lewisite; ΔX =X($B_{12}N_{12}$… Lewisite) – X($B_{12}N_{12}$) - X(Lewisite); X=G, H, S

$M^+@B_{12}N_{12}$ + Lewisite → $M^+@B_{12}N_{12}$… Lewisite; ΔX =X($M^+@B_{12}N_{12}$… Lewisite) – X($M^+@B_{12}N_{12}$)-X(Lewisite); X=G, H, S

The computed parameters are recorded in Table 3. The negative ΔG and ΔH values of the $B_{12}N_{12}$… Lewisite and $M^+@B_{12}N_{12}$… Lewisite complexes uncovered that the examined responses are spontaneous and exothermic, respectively. The negative ΔS values of these responses are consistent. The arrangement of the particles diminished the entropy of the reaction after the interaction between two molecules. The more negative values of ΔG and ΔH indicated more spontaneous and exothermic responses of $M^+@B_{12}N_{12}$… Lewisite complexes arrangement than $B_{12}N_{12}$… Lewisite complex. ΔG and ΔH values are diminished with

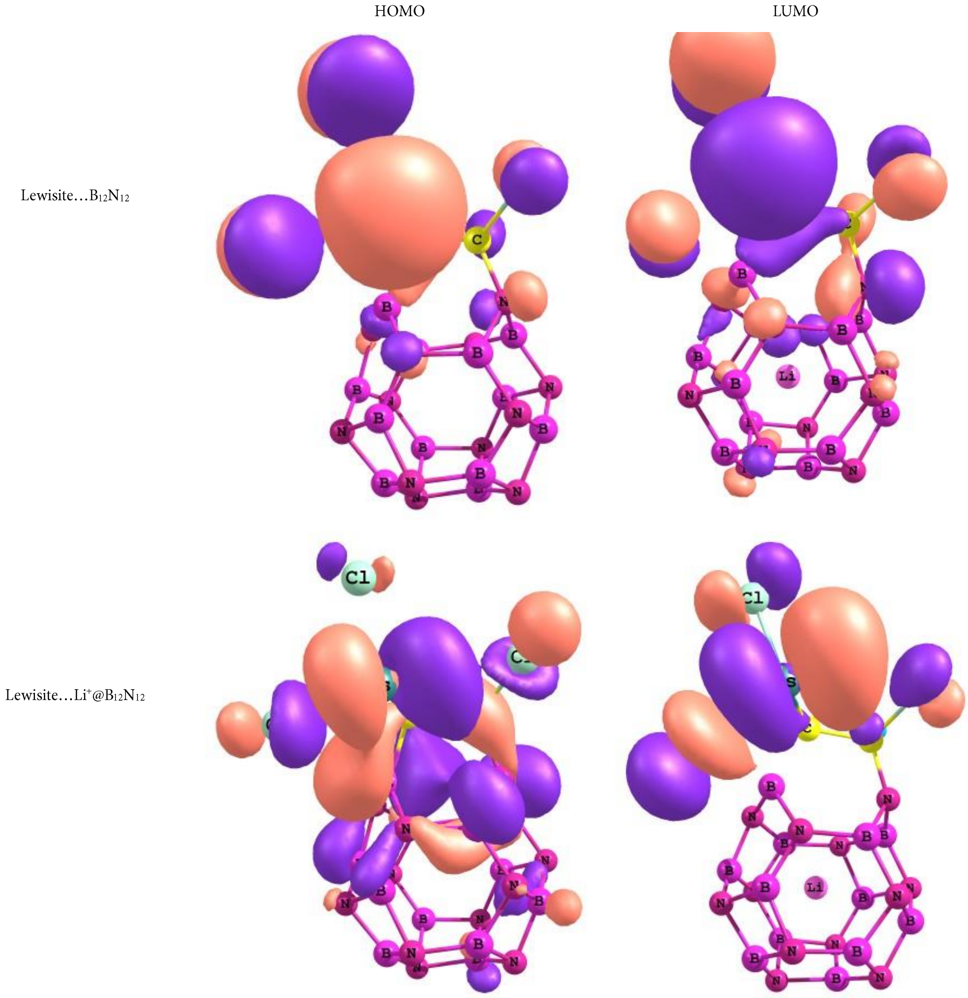

Fig. 2. Plots of frontier orbitals in the $B_{12}N_{12}$… Lewisite and $Li^+@B_{12}N_{12}$… Lewisite systems.

expanding of the nuclear effective charge of M^+.

Formation constant values (K) of the arrangement of these complexes are calculated by following formula:

$$\Delta G=-nRT\ \ln K$$

The computed K values are recorded in Table 3. Larger values for $M^+@B_{12}N_{12}$… Lewisite complexes than $B_{12}N_{12}$… Lewisite complex can be seen. These values increment with increasing of the nuclear efficient charge of M^+.

CONCLUSION

Computational examination of adsorption of Lewisite warfare agent on the $B_{12}N_{12}$ and $M^+@B_{12}N_{12}$ ($M^+ = Li^+, Na^+, K^+$) nano-clusters with LC-wPBE/ 6-311+G(d,p) at the level of theory showed the doped nano-clusters had more propensity to adsorb Lewisite than $B_{12}N_{12}$ cluster. Appropriation strength decreased with increasing of effective atomic number of metal cation. Lewisite fragment had important commitment within the frontier orbitals of examined systems. Responses of $M^+@B_{12}N_{12}$… Lewisite complexes arrangement was more spontaneous and exothermic than $B_{12}N_{12}$… Lewisite complex.

REFERENCES

1. Marrs TC, Maynard RL, Sidell FR, Chemical Warfare Agents: Toxicology and Treatment. Wiley: New York, 1996.
2. Green SJ, Price TWI, The Chlorovinylchloroarsines. J. Chem. Soc. Trans. , 1921; 119: 448–453. https://doi.org/10.1039/CT9211900448
3. Webb JL, Arsenicals; Enzyme and Metabolic Inhibitors. Academic Press: New York, 1966; Vol. 3.

4. Szekeres LI, Gyurcsik B, Kiss T, Kele Z, Jancsó A, Interaction of Arsenous Acid with the Dithiol-Type Chelator British Anti-Lewisite (BAL): Structure and Stability of Species Formed in an Unexpectedly Complex System. Inorganic Chemistry, 2018; 57: 7191-7200. https://doi.org/10.1021/acs.inorgchem.8b00894
5. Sahu C, Pakhira S, Sen K, Das AK, A Computational Study of Detoxification of Lewisite Warfare Agents by British Anti-lewisite: Catalytic Effects of Water and Ammonia on Reaction Mechanism and Kinetics. J. Phys. Chem. A, 2013; 117: 3496–3506. https://doi.org/10.1021/jp312254z
6. Strout DL, Structure and Stability of Boron Nitrides: Isomers of B12N12. J. Phys. Chem. A 2000; 104: 3364-3366. https://doi.org/10.1021/jp994129a
7. Wang R, Zhang D, Liu C, Theoretical prediction of a novel inorganic fullerene-like family of silicon-carbon materials. Chem. Phys. Lett., 2005; 411: 333-338. https://doi.org/10.1016/j.cplett.2005.06.055
8. Bertolus B, Finocchi F, Millie P, Investigating bonding in small silicon-carbon clusters: exploration of the potential energy surfaces of Si3C4, Si4C3, and Si4C4 using ab initio molecular dynamics. J. Chem. Phys., 2004; 120: 4333-4343. https://doi.org/10.1063/1.1636717
9. Fu C-C, Weissmann M, Machado M, Ordejón P, Ab initio study of silicon-multisubstituted neutral and charged fullerenes. Phys. Rev. B 2001; 63: 85411. https://doi.org/10.1103/PhysRevB.63.085411
10. Kandalam AK, Blanco MA, Pandey R, Theoretical Study of Structural and Vibrational Properties of Al3N3, Ga3N3, and In3N3. J. Phys. Chem. B, 2001; 105: 6080-6084. https://doi.org/10.1021/jp004404p
11. Tahmasebi ESE, Biglari Z, Theoretical assessment of the electro-optical features of the group III nitrides (B12N12, Al12N12 and Ga12N12) and group IV carbides (C24, Si12C12 and Ge12C12) nanoclusters encapsulated with alkali metals (Li, Na and K). Appl. Surf. Sci., 2016; 363: 197-208. https://doi.org/10.1016/j.apsusc.2015.12.001
12. Zhang QWF, Wang X, Liu N, Yang J, Hu Y, Yu L, Hu Z, Zhu J, 6-Fold-Symmetrical AlN Hierarchical Nanostructures: Synthesis and Field-Emission Properties. J. Phys. Chem. C, 2009; 113: 4053-4058. https://doi.org/10.1021/jp811484r
13. Wu H-S, Zhang F-Q, Xu X-H, Zhang C-J, Jiao H, Geometric and Energetic Aspects of Aluminum Nitride Cages. J. Phys. Chem. A, 2003; 107: 204-209. https://doi.org/10.1021/jp027300i
14. Wu H, Fan X, Kuo J-L, Metal free hydrogenation reaction on carbon doped boron nitride fullerene: A DFT study on the kinetic issue. Int. J. Hydrogen Energy, 2012; 37: 14336-14342. https://doi.org/10.1016/j.ijhydene.2012.07.081
15. Kim KK, Hsu A, Jia X, Kim SM, Shi Y, Hofmann M, Nezich D, Rodriguez-Nieva JF, Dresselhaus M, Palacios T, Synthesis of monolayer hexagonal boron nitride on Cu foil using chemical vapor deposition. Nano letters, 2011; 12: 161-166. https://doi.org/10.1021/nl203249a
16. Ciofani G, Genchi GG, Liakos I, Athanassiou A, Dinucci D, Chiellini F, Mattoli V, A simple approach to covalent functionalization of boron nitride nanotubes. Journal of colloid and interface science, 2012; 374: 308-314. https://doi.org/10.1016/j.jcis.2012.01.049
17. Oku T, Nishiwaki A, Narita I, Sci. Technol. Adv. Mater, 2004; 5: 635-. https://doi.org/10.1016/j.stam.2004.03.017
18. Oku T, Narita I, Nishiwaki A, Mater. Manuf. Process. , 2004; 19: https://doi.org/10.1081/LMMP-200035336
19. Baei MT, Taghartapeh MR, Lemeski ET, Soltani A, A computational study of adenine, uracil, and cytosine adsorption upon AlN and BN nano-cages. Physica B 2014; 444: 6-13. https://doi.org/10.1016/j.physb.2014.03.013
20. Rad AS, Ayub K, Adsorption of pyrrole on Al12N12, Al12P12, B12N12, and B12P12 fullerene-like nano-cages; a first principles study. Vacuum 2016; 131: 135-141. https://doi.org/10.1016/j.vacuum.2016.06.012
21. Soltani A, Baei MT, Lemeski ET, Shahini M, Sensitivity of BN nano-cages to caffeine and nicotine molecules. Superlattices and Microstructures 2014; 76: 315-325. https://doi.org/10.1016/j.spmi.2014.09.031
22. Vessally E, Esrafili MD, Nurazar R, Nematollahi P, Bekhradnia A, A DFT study on electronic and optical properties of aspirin-functionalized B12N12 fullerene-like nanocluster. Structural Chemistry, 2017; 28: 735-748. https://doi.org/10.1007/s11224-016-0858-y
23. S.Onsori, Alipour E, A computational study on the cisplatin drug interaction with boron nitride nanocluster. Journal of Molecular Graphics and Modelling, 2018; 79: 223-229. https://doi.org/10.1016/j.jmgm.2017.12.007
24. Soltani A, Sousaraei A, Javan MB, Eskandaric M, Balakheylid H, Electronic and optical properties of 5-AVA-functionalized BN nanoclusters: a DFT study New J. Chem., 2016; 40: 7018-7026. https://doi.org/10.1039/C6NJ00146G
25. Frisch MJ, Trucks GW, Schlegel HB, Scuseria GE, Robb MA, Cheeseman JR, Scalman G, Barone V, Mennucci B, Petersson GA, Nakatsuji H, Caricato M, Li X, Hratchian HP, Izmaylov AF, Bloino J, Zheng G, Sonnenberg JL, Hada M, Ehara M, Toyota K, Fukuda R, Hasegawa J, Ishida M, T. Nakajima, Honda Y, Kitao O, Nakai H, Vreven T, Montgomery JA, Jr., Peralta JE, Ogliaro F, Bearpark M, Heyd JJ, Brothers E, Kudin KN, Staroverov VN, Kobayashi R, J. Normand, Raghavachari K, Rendell A, Burant JC, Iyengar SS, J. Tomasi, Cossi M, Rega N, Millam JM, Klene M, Knox JE, Cross JB, Bakken V, Adamo C, Jaramillo J, Gomperts R, Stratmann RE, Yazyev O, Austin AJ, Cammi R, Pomelli C, Ochterski JW, Martin RL, Morokuma K, Zakrzewski VG, Voth GA, Salvador P, Dannenberg JJ, Dapprich S, Daniels AD, Farkas O, Foresman JB, Ortiz JV, Cioslowski J, Fox DJ Gaussian 09, Revision A.02; Gaussian, Inc.: Wallingford CT, 2009.
26. Krishnan R, Binkley JS, Seeger R, Pople JA, Self-consistent molecular orbital methods. XX. A basis set for correlated wave functions. J. Chem. Phys., 1980; 72: 650. https://doi.org/10.1063/1.438955
27. McLean AD, Chandler GS, Contracted Gaussian basis sets for molecular calculations. I. Second row atoms, Z=11-18. J. Chem. Phys., 1980; 72: 5639. https://doi.org/10.1063/1.438980
28. Curtiss LA, McGrath MP, Blandeau J-P, Davis NE,

Binning RC, Radom JL, Extension of Gaussian-2 theory to molecules containing third-row atoms Ga-Kr. J. Chem. Phys., 1995; 103: 6104. https://doi.org/10.1063/1.470438

29. Vydrov OA, Scuseria GE, Assessment of a long-range corrected hybrid functional. J. Chem. Phys., 2006; 125: 234109. https://doi.org/10.1063/1.2409292
30. Breneman CM, Wiberg KB, Determining atom-centered monopoles from molecular electrostatic potentials - the need for high sampling density in formamide conformational-analysis. J. Comp. Chem., 1990; 11: 361-373. https://doi.org/10.1002/jcc.540110311
31. S. Simon MD, Dannenberg JJ, How does basis set superposition error change the potential surfaces for hydrogen bonded dimers? J. Chem. Phys., 1996; 105: 11024-11031. https://doi.org/10.1063/1.472902